THE JOURNAL OF BIOLOGICAL CHEMISTRY VOL. 285, NO. 34, pp. 26199–26210, August 20, 2010

Erk5 Activation Elicits a Vasoprotective Endothelial Phenotype via Induction of Krüppel-like Factor 4 (KLF4)*[S]

Received for publication, January 12, 2010, and in revised form, June 2, 2010 Published, JBC Papers in Press, June 15, 2010, DOI 10.1074/jbc.M110.103127

Nils Ohnesorge[‡‖], Dorothee Viemann[§], Nicole Schmidt[‡], Tobias Czymai[‡], Désirée Spiering[¶], Mirco Schmolke[¶], Stephan Ludwig[¶], Johannes Roth[§], Matthias Goebeler[‡‖1], and Marc Schmidt[‡‖1,2]

From the [‡]Department of Dermatology, University Hospital Mannheim, University of Heidelberg, Mannheim 68167, Germany, the [§]Institutes for Immunology and Molecular Virology and [¶]Center of Molecular Biology of Inflammation (ZMBE), University of Muenster, Muenster 48149, Germany, and the [‖]Department of Dermatology, University Hospital Giessen, University of Giessen, Giessen 35392, Germany

The MEK5/Erk5 MAPK cascade has recently been implicated in the regulation of endothelial integrity and represents a candidate pathway mediating the beneficial effects of laminar flow, a major factor preventing vascular dysfunction and disease. Here we expressed a constitutively active mutant of MEK5 (MEK5D) to study the transcriptional and functional responses to Erk5 activation in human primary endothelial cells. We provide evidence that constitutive Erk5 activation elicits an overall protective phenotype characterized by increased apoptosis resistance and a decreased angiogenic, migratory, and inflammatory potential. This is supported by bioinformatic microarray analysis, which uncovered a statistical overrepresentation of corresponding functional clusters as well as a significant induction of anti-thrombotic, hemostatic, and vasodilatory genes. We identify KLF4 as a novel Erk5 target and demonstrate a critical role of this transcription factor downstream of Erk5. We show that KLF4 expression largely reproduces the protective phenotype in endothelial cells, whereas KLF4 siRNA suppresses expression of various Erk5 targets. Additionally, we show that vasoprotective statins potently induce KLF4 and KLF4-dependent gene expression via activation of Erk5. Our data underscore a major protective function of the MEK5/Erk5/KLF4 module in ECs and implicate agonistic Erk5 activation as potential strategy for treatment of vascular diseases.

The vascular endothelium, located at the interface between blood and tissue, fulfills a plethora of important functions, including the supply of nutrients and oxygen to the surrounding tissues as well as regulation of hemostasis and inflammatory responses. Endothelial dysfunction contributes to several diseases including chronic inflammation, hemophilia, thrombosis, and atherosclerosis. Thus, elucidation of the factors and molecular mechanisms that influence endothelial function is essential for the development of novel prophylactic and therapeutic strategies against diseases involving the vascular system. A major determinant influencing endothelial integrity is the hemodynamic force exerted by steady pulsatile blood flow. This force generates a continuous shear stress on the endothelial cells (ECs)[3] in the vessel wall, resulting in gene expression changes that protect the vessel from excessive inflammatory responses and thrombosis and provides an essential survival and quiescence signal for the vascular endothelium (1).

Various signaling pathways and transcription factors are involved in perception and mediation of shear stress responses. These include the MEK5/Erk5 mitogen-activated protein kinase (MAPK) pathway (2), which is activated by laminar shear stress in ECs (3). In analogy to the related Erk1/2 MAPK, Erk5 activation is triggered by dual phosphorylation at a TEY consensus motif by a mitogen-activated protein kinase kinase (MAPKK or MEK), which in turn is activated via phosphorylation by a MEK kinase (MEKK or MAP3K) (4). In the case of Erk5, the activating phosphorylation is executed by MEK5. Its interaction with Erk5 is mediated via a unique Phox and Bem1 (PB1) protein dimerization/oligomerization domain that discriminates MEK5 from related MAPK kinases and confers specificity to the reaction (5). Upon activation, Erk5 shuttles to the nucleus and stimulates transcription through direct phosphorylation of transcription factors such as MEF2C (6). Additionally, Erk5 can directly influence transcription via a poorly defined alternative mechanism that requires the presence of a unique C-terminal domain, which is absent in other MAPKs (7). Recent knock-out studies revealed an indispensable role of the MEK5/Erk5 cascade in embryonic vascular development and maintenance of vascular integrity in mature blood vessels (2, 8–10). Erk5 further was shown to mediate shear stress-dependent repression of inflammatory responses via interaction with PPARγ1 (11) and regulates flow-mediated expression of KLF2 (12), a mechano-activated transcription factor that controls various vasoprotective, anti-thrombotic, and anti-inflammatory responses to laminar flow (12–15). However, Erk5 is

* This work was funded by Deutsche Forschungsgemeinschaft Grants GO 811/1-5 (to M. G.) and GRK880/3 (International Research Training Group Vascular Medicine, Graduiertenkolleg 880/3 (to M. S. and M. G.)).

[S] The on-line version of this article (available at http://www.jbc.org) contains supplemental.

[1] Both authors shared senior authorship.

[2] To whom correspondence should be addressed: Dept. of Dermatology, University of Giessen, Gaffkystrasse 14, 35392 Giessen, Germany. Tel.: +49-641-99-43210; Fax: +49-641-99-43219; E-mail: marc.schmidt@derma.med.uni-giessen.de.

[3] The abbreviations used are: EC, endothelial cell; MEK, mitogen-activated protein kinase kinase/extracellular signal-regulated kinase kinase; Erk, extracellular signal-regulated kinase; MAPK, mitogen-activated protein kinase; TNF, tumor necrosis factor; VEGF, vascular endothelial growth factor; siRNA, small interfering RNA; shRNA, small hairpin RNA; qRT, quantitative real-time PCR; PI, propidium iodide; HUVEC, human umbilical cord endothelial cell; THBD, thrombomodulin; CBP cAMP-response element-binding protein (CREB)-binding protein; KLF4, Krüppel-like factor 4; PLAT, tissue plasminogen activator.

also stimulated by growth factors (2) and stress stimuli such as hyperosmolarity or oxidative stress in various cells (6, 16), raising questions about the relevant physiological stimuli and downstream consequences of vascular Erk5 activation.

The accumulation of data implicating Erk5 as mediator of flow-induced responses prompted us to analyze the effect of active Erk5 on the endothelial transcriptional program and distinct protective functions under static conditions. We provide evidence that sustained activation of the Erk5 pathway by expression of a constitutively active MEK5 mutant (MEK5D) elicits a protective gene expression pattern resulting in an anti-angiogenic, anti-inflammatory, and anti-apoptotic phenotype in human primary ECs. We reveal Krüppel-like factor 4 (KLF4) as a protective factor downstream of Erk5 and demonstrate that vasoprotective drugs of the statin family potently activate the MEK5/Erk5/KLF4 pathway. Our data suggest the MEK5/Erk5/KLF4 module as an important regulator of endothelial function and underscore the therapeutic potential of agonists of this pathway for diseases associated with vascular dysfunction.

EXPERIMENTAL PROCEDURES

Reagents—Human recombinant tumor necrosis factor-α (TNF) and vascular endothelial growth factor (VEGF) were obtained from R&D Systems and used at a concentration of 2 or 10 ng/ml, respectively. Monensin was purchased from Applichem and statins were from Calbiochem and used at 2 or 10 μM, respectively. All other reagents were purchased from Sigma unless stated otherwise.

Small Interfering RNA (siRNA)—The following siRNAs were ordered from Applied Biosystems (Ambion): siErk5 (110792), siKLF2a (116130), siKLF2b (s20270), siKLF4 (s17794). The siRNA against MEK5 was purchased from Qiagen (SI00300713). The negative control of scrambled siRNA was synthesized by MWG with the sequence UCUCCGAACGUGUCACGUtt.

Antibodies—The following primary antibodies were used for Western blot: ADAMTS1 (268104), NOV/CCN3 (AF1640) (R&D Systems), cleaved Caspase-3 (9664), phospho-Erk1/2 (p44/p42) (9101) (Cell Signaling), eNOS/NOS Type III (610298, BD Biosciences), Erk5 (07-039, Upstate Biotechnology), IκB (SC-371), KLF4 (SC-20691), MEK5 (SC-10795), PAI2 (3750, American Diagnostics), α-tubulin (B-5-1-2), and FLAG (M2, Sigma).

Plasmids—A retroviral construct for stable expression of constitutively active rat MEK5-α1 (pBP-MEK5D) was generated by subcloning a 5′ blunt-ended KpnI/SalI fragment from CMV-MEK5D-HA (6) into the SnaBI and SalI sites of the retroviral expression vector pBabe puro (pBP) upon which the C-terminal hemagglutinin tag was lost. The stop codon was then reinserted by site-directed mutagenesis (QuikChange II site-directed mutagenesis kit; Stratagene). An expression vector for human KLF4 was purchased from Origene and subcloned by EcoRI digest into pBabe puro. pEGZ expression vectors for wild-type human FLAG-Erk5 and dominant-negative flag-Erk5-AEF have been described before (17). For retroviral expression of small hairpin RNA (shRNA) against Erk5, a 64-mer DNA oligonucleotide containing the specific 19-mer targeting sequence GAGTCACCTGATGTCAACC for human and mouse Erk5 was cloned into the BamHI/HindIII sites of the pRetro Super puro (pRS) shRNA expression vector (18).

Cell Culture and Retroviral Infections—Human U2OS osteosarcoma cells were cultured in Dulbecco's modified Eagle's medium (Gibco® Invitrogen) containing 10% fetal bovine serum (PAA) and transfected by calcium phosphate according to standard procedures. Human umbilical cord endothelial cells (HUVECs) were purchased from Promocell and cultured as described (19). Retroviral infection of HUVECs was carried out in two consecutive rounds as detailed before (20). Cells were used unselected for RNA isolation and for kinetic experiments. Alternatively, infected cells were selected for puromycin resistance conferred by the retroviral backbone 72 h post-infection (2 μg/ml puromycin, overnight) and reseeded into puromycin-free medium for the experiments.

siRNA Transfection—HUVECs were transfected with the different siRNAs as described (19). After transfection, HUVECs were incubated for 4 h at 37 °C and infected with the indicated retroviruses. Lysates were taken 50 h after transfection (*i.e.* 40 h after the second infection). Alternatively, uninfected cells were stimulated with 10 μM simvastatin the day after transfection and lysed 24 h later.

Quantitative Real-time PCR (qRT-PCR)—RNA was isolated using RNeasy Minikit (Qiagen), and 1 μg RNA was transcribed into cDNA employing the Transcriptor High Fidelity cDNA Synthesis Kit (Roche Applied Science). For single genes, TaqMan gene expression assays were purchased from Applied Biosystems (for glyceraldehyde-3-phosphate dehydrogenase (hs99999905_m1), KLF2 (hs00360439_g1), KLF4 (hs00358836_m1), and VCAM1 (hs003369_m1)). Otherwise, qRT-PCRs were performed using the SYBER Green method as described (20). Primer sequences are available upon request. Expression of all genes was normalized by comparison to expression of glyceraldehyde-3-phosphate dehydrogenase. Unless indicated, RNA lysates for qRT-PCR were taken 40 h post-second infection.

Microarray Analysis—HUVEC were infected in three independent experiments with either empty pBP vector or pBP-MEK5D in two consecutive rounds. 40 h after the second infection, total RNA was isolated and individually processed for microarray hybridization using Affymetrix HG-U133 Plus 2.0 arrays according to the manufacturer's instructions (Affymetrix, Santa Clara, CA).

Microarray data were analyzed using MicroArray Suite (MAS) Software 5.0 (Affymetrix). First, background-adjusted raw intensities accounting for nonspecific binding by removing probe sets with insignificant differences between single perfect-matching (PM) and mismatching (MM) probes were created. Single raw values were calculated for each probe set from the median of PM/MM discrimination values. -Fold changes (log ratio changes) and "change in *p* values" based on a signed rank test were determined for each experiment. Only genes with a change $p \leq 0.05$ for up-regulated or a change $p \geq 0.95$ for down-regulated genes in at least 2 of 3 experiments and mean log ratio changes (calculated as mean of log ratio changes of all experiments with significant change *p* values) of at least 2.0 or −2.0 compared with the empty vector were considered.

Functional Annotation Clustering—Functional annotation clustering was performed employing a functional annotation clustering tool from the Data base for Annotation, Visualization, and Integrated Discovery (DAVID) (david.abcc.ncifcrf.gov) using the parameters Affymetrix HG-U133_Plus_2 as background, *Homo sapiens* as species, GOTERM_BP_ALL for gene ontology, and "high" as the level of classification stringency (21).

Western Blot—HUVECs were lysed, and equal amounts of protein were subjected to reducing SDS-PAGE as described (20) except for ADAMTS1, which was analyzed by native PAGE. Protein expression was then analyzed by immunoblot as described (20).

Quantification of Subdiploidy—To analyze cellular apoptosis upon growth factor withdrawal, puromycin-selected HUVECs were reseeded at a density of 3.5×10^5/10-cm dish and incubated in medium with or without growth factors for 48 h. Culture supernatants and trypsinized cell pellets were pooled, washed with phosphate-buffered saline, and fixed for 1 h with ice-cold 70% ethanol before staining with 10 μg/ml propidium iodide (PI) and 250 μg/ml RNase. Cell cycle distribution and quantity of subdiploidy of the PI-stained cells was then analyzed flow-cytometrically by linear measurement of PI-A fluorescence.

Three-dimensional Matrix Gel Sprouting Assay—HUVECs were grown to confluence and reseeded in hanging drops of 25 μl of medium containing 1000 cells and 12 g/liter methylcellulose. The following day, spheroids were seeded in a collagen matrix and incubated in medium 199 with or without 10 ng/ml VEGF for 24 h. Cells were fixed with 10% paraformaldehyde, and the total sprouting length from each 10 spheroids was measured on microscopic images taken at 200× magnification using Leica Image Manager IM50 software (Version 1.20).

Migration Assays—Migration assays were essentially performed as described (22). Briefly, 1.0-mm-thick steel plates were inserted into wells before seeding to produce a cell-free space. After removal of the steel plate, migration into the cell-free space was monitored by inverted microscopy. Images were taken at 0 and 16 h to calculate migration distance.

Leukocyte Adhesion Assay—HUVECs were grown in six wells and stimulated with 2 ng/ml TNF overnight. Thereafter, exponentially growing THP-1 monocytes were labeled with the green-fluorescent dye CFSE (CellTRace CFSE Cell Proliferation kit, Invitrogen) and resuspended in endothelial growth medium at a density of 2×10^5 cells/ml. After removal of the stimulation medium, HUVECs were overlaid with 1 ml of monocyte suspension and immediately tumbled for 10 min at 60 rpm. Non-attached monocytes were removed by three rinses with phosphate-buffered saline, and bound monocytes were visualized by fluorescence microscopy. For quantitative determination of monocyte attachment, cells were lysed in 0.1% NaOH, 0.01% SDS in double distilled H_2O, and fluorescence intensities were measured at 488 nm with reference filter 517 nm.

Enzyme-linked Immunosorbent Assay—For the quantification of released interleukin-8 and MCP1 in the supernatants of the differently infected and stimulated cells, OptEIA enzyme-linked immunosorbent assay kits (BD Pharmingen) were used according to the manufacturer's instructions. HUVECs were stimulated with 2 ng/ml TNF for 6 h in all experiments.

Luciferase Assays—Luciferase assays using a 6× NFκB-luciferase construct and an ubiquitin-dependent renilla luciferase reporter as reference were performed as described (19).

Fluorescence-activated Cell Sorter Staining—For surface detection of VCAM1, fluorescence-activated cell sorter staining was performed essentially as described (23). For statistical analysis, median fluorescence intensity (MFI) ratios were calculated between the measured median fluorescence intensity values of the respective antibody-stained protein of interest and the IgG1-stained controls, and -fold changes in MFI ratios of TNF-stimulated and unstimulated controls were calculated from at least three independent experiments and presented ±S.D.

Statistical Analysis—The mean of at least three individual experiments was calculated, and error bars were given to indicate the S.D. An unpaired Student's t test was calculated to determine significance of the values. p values of less than 0.05 were considered significant and are indicated by an *asterisk*.

RESULTS

Static Erk5 Activation Elicits a Protective Phenotype in Human Primary Endothelial Cells—Laminar flow confers various protective capacities to ECs. To investigate whether static Erk5 activation can mimic at least some of these aspects of laminar flow, we employed a constitutively active mutant of its upstream kinase MEK5, MEK5D (6). Retroviral transduction of this mutant into primary HUVECs triggered a rapid electromobility shift in Erk5 to a slower migrating form, which was evident as early as 16–24 h after infection and reached its maximum at about 40 h (Fig. 1*A*). This band corresponded to phosphorylated Erk5 as it was missing in co-transfection experiments of MEK5D with an Erk5 variant lacking the phosphorylation sites for MEK5 (Erk5-AEF; Fig. 1*B*). In agreement with published results (22), MEK5D expression had no effect on phosphorylation of the closely related MAPKs Erk1 and -2, confirming specificity of MEK5 for Erk5.

Having confirmed functionality of the MEK5D mutant, we tested its effect on endothelial survival. ECs infected with either empty vector or MEK5D were analyzed regarding their sensitivity to apoptosis induction by growth factor deprivation. Stable MEK5D expression strongly decreased both basal and starvation-induced apoptosis as evident by a reduced percentage of cells with a subdiploid DNA content in DNA profiling experiments. This anti-apoptotic effect was strictly dependent on Erk5 as shRNA-mediated depletion of Erk5 could restore the sensitivity to growth factor deprivation (Fig. 1*C*).

To uncover a potential anti-angiogenic and anti-migratory effect of Erk5 activation, we employed a three-dimensional spheroid model. Compared with vector-infected cells, spheroids of HUVECs stably expressing MEK5D showed markedly decreased basal and VEGF-induced sprouting (Fig. 1*D*).

Finally, we explored whether MEK5D expression also influences inflammatory responses. Vector- and MEK5D-infected HUVECs were subjected to an *in vitro* monocyte adhesion assay in which the differently transfected ECs were stimulated with TNF and subsequently examined for adhesion of fluorescently

labeled THP-1 monocytes. Indeed, expression of MEK5D strongly inhibited TNF-induced monocyte adhesion (Fig. 1*E*). This occurred in an Erk5-dependent manner as co-infection of shRNA against Erk5 reversed this effect (Fig. 1*F*). Taken together these results indicate that Erk5 activation mimics various beneficial effects of laminar flow under static conditions.

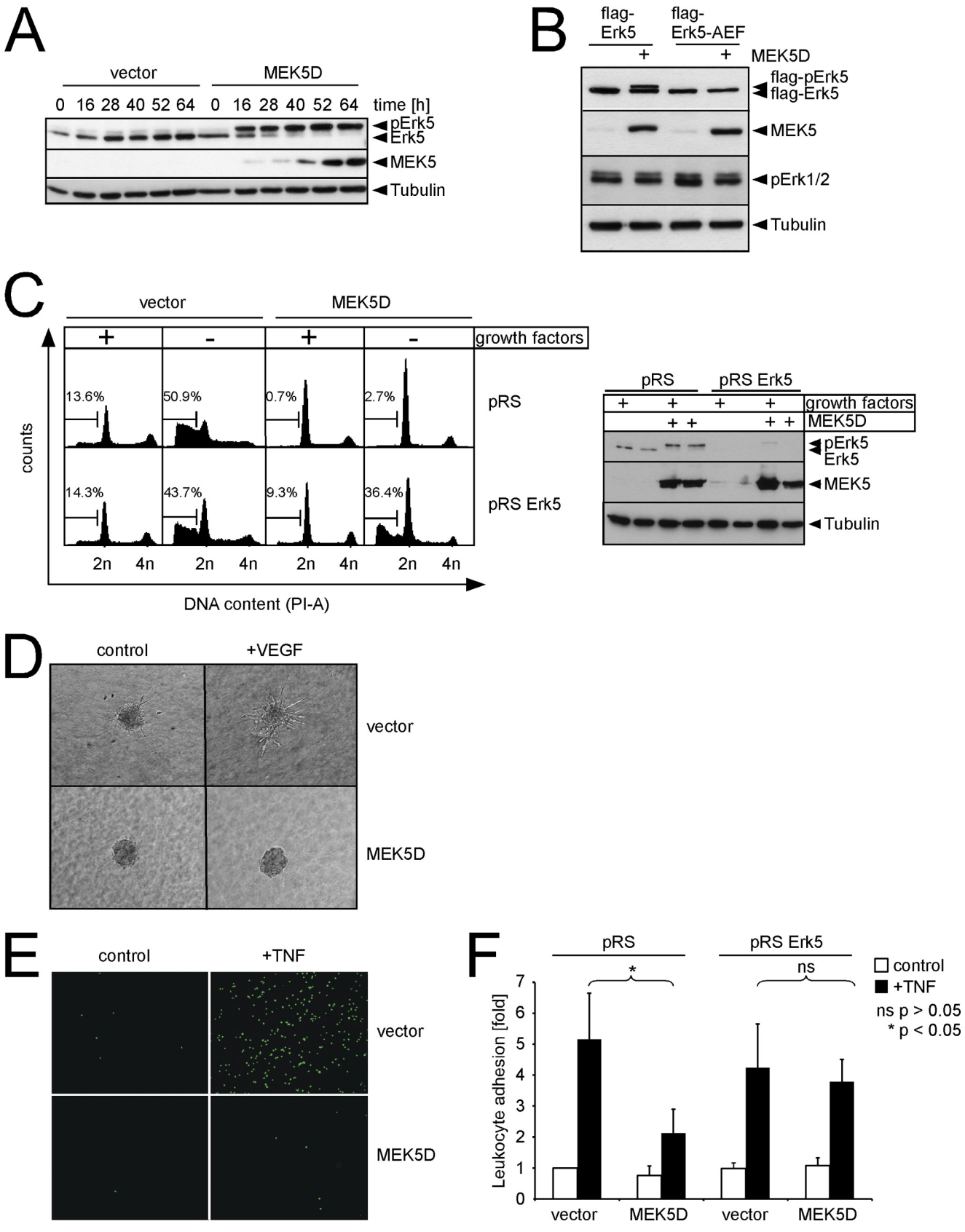

Transcriptional Targets of the MEK5/Erk5 Cascade—We next performed a global gene expression analysis using the Affymetrix gene chip platform to gain better insight into the molecular mechanisms by which active Erk5 mediates its protective effects. HUVECs infected with empty vector or constitutively active MEK5D were processed for microarray analysis. mRNA was obtained at 40 h post-infection as kinetic experiments reproducibly showed a maximal Erk5 phosphorylation at this time point (Fig. 1*A*). Comparison of the mRNA profiles of MEK5D-expressing HUVECs to those of vector-infected cells overall revealed 239 genes that were at least 2-fold regulated, consisting of 172 up-regulated or newly induced transcripts and 67 repressed genes. The set of up-regulated transcripts contained various well known protective genes and transcripts previously found to be induced by laminar flow such as the established Erk5 target KLF2, NOS3/eNOS, the drug-metabolizing and detoxifying cytochrome p450 family member Cyp1B1, the anti-coagulant gene CD59, or arginosuccinate synthase, a rate-limiting enzyme regulating NOS3 substrate availability (supplemental Table S2; microarray data are further deposited at Gene Expression Omnibus under accession number GSE17939). In qRT-PCR experiments we could validate statistically significant regulation for all of nine selected target genes by MEK5D, confirming the reliability of our microarray data (Fig. 2*A*).

We next performed functional annotation clustering using a freely accessible tool from the Data base for Annotation, Visualization, and Integrated Discovery (DAVID; david.abcc.ncifcrf.gov). This tool collects available functional information for the individual genes from a regulated dataset (in this case, the identified MEK5D-regulated transcripts of our microarray) according to entries in the gene ontology (GO) data base, which classifies all genes of known or implied function into hierarchical GO groups. In a second step this tool then integrates this information by grouping genes with functionally similar GO group entries into functional annotation clusters. For each of these functional clusters it then calculates an enrichment score, which is based on the *p* values for coincidental distribution determined for the included GO-groups and represents a value describing the overrepresentation of genes with similar function among a given dataset (21). For both up- and down-regulated transcripts, we overall identified six functional clusters containing GO groups with statistically significant *p* values (<0.05) (Fig. 2*B*). Besides clusters related to migration such as "Cell morphogenesis," "G-protein signaling," "Actin cytoskeleton reorganization," and "Cell migration/motility," which contained prominent anti-migratory genes for ECs such as SEMA3F (24, 25) (supplemental Tables S1 and S4), analysis of the up-regulated genes also revealed clusters related to "Regulation of blood pressure/vasodilatation" and "Blood coagulation/hemostasis." (Fig. 2*B*). The latter contained various anti-thrombotic genes such as thrombomodulin (THBD), tissue plasminogen activator (PLAT/t-PA), or CD59, suggesting a potential anti-thrombotic effect of constitutive Erk5 activation (supplemental Table S1). Among the down-regulated transcripts, especially functional gene clusters related to inflammation and chemotaxis-containing genes such as the proinflammatory cytokines interleukin-8 and MCP1/CCL2 were overrepresented, indicative of a global suppressive effect of the MEK5/Erk5 cascade on endothelial inflammation (supplemental Table S1).

Transcription Factors Downstream of Erk5—We next screened our gene lists for potential downstream transcription factors that could elicit the described gene responses. Consistent with earlier studies that established KLF2 as Erk5 target (12, 26), we found KLF2 among the top-regulated genes in HUVEC (supplemental Table S3). Besides KLF2, however, we also identified another Krüppel-like factor, KLF4. Interestingly, KLF4 has recently been reported as a shear stress-activated gene and an important regulator of inflammation in ECs (27, 28). Thus, KLF4 was a good candidate to mediate at least some of the gene expression downstream of Erk5. Fig. 2*C* illustrates that MEK5D expression triggered a pronounced KLF4 protein induction in HUVEC. siRNA experiments revealed that this was not dependent on KLF2 as transfection of MEK5D-infected cells with two different siRNAs for KLF2 had no effect on KLF4 expression by MEK5D but readily reduced induction of NOS3, a known KLF2 target (Fig. 2*D*) (12, 13). In contrast, transfection of either a siRNA against KLF4 or Erk5 reduced KLF4 protein expression to basal levels (Fig. 2*D*). Strikingly, we also observed an almost complete inhibition of MEK5D-induced NOS3 protein expression upon KLF4 depletion. To exclude a potential regulation of KLF2 by KLF4, we performed qRT-PCRs. Fig. 2*E* illustrates that KLF4 depletion had no significant effect on MEK5D-induced KLF2 expression. Conversely, KLF2 depletion did not significantly reduce KLF4 expression, whereas Erk5 siRNA inhibited induction of both transcripts efficiently (Fig. 2*E*). Thus, Erk5 regulates expression of KLF2 and KLF4 independently of each other.

KLF4 Mediates Gene Expression Downstream of Erk5 in ECs—The finding that Erk5-induced NOS3 expression is reduced by

FIGURE 1. **MEK5D expression elicits an anti-apoptotic, anti-angiogenic, and anti-inflammatory phenotype in human EC.** *A*, HUVECs were infected with either an empty retrovirus or a retrovirus encoding MEK5D. At the indicated time points after infection, cells were lysed and analyzed for Erk5 phosphorylation and MEK5D expression by immunoblot using antisera against Erk5 or MEK5, respectively. Tubulin served as the loading control. *B*, U2OS osteosarcoma cells were co-transfected with pBP-MEK5D and FLAG-wt-Erk5 or MEK5-insensitive FLAG-Erk5-AEF, and phosphorylation and expression of the indicated proteins was detected by immunoblot using antibodies against MEK5, FLAG, phospho-Erk1/2, and tubulin (as loading control). *C–F*, HUVECs were infected with the indicated retroviruses. Except for *D*, cells were puromycin-selected and reseeded for the respective assays. *C*, *left panel*, shown is flow cytometric quantification of subdiploid DNA content (indicating apoptosis) of PI-stained cells cultured in presence or absence of growth factors for 48 h. Co-expression of Erk5 shRNA *(pRS-Erk5*) reverses the anti-apoptotic effect of active MEK5D. *Right panel*, shown is a Western blot, confirming MEK5D protein expression and knockdown efficiency of the Erk5 shRNA construct. An immunoblot for tubulin was included as loading control. *D*, decreased basal and VEGF-induced angiogenic sprouting of MEK5D-infected HUVEC in a three-dimensional *in vitro* sprouting assay 24 h after incubation in VEGF-free or VEGF-containing (10 ng/ml) medium. *E*, a fluorescence microscopy image shows decreased adhesion of fluorochrome-labeled THP-1 monocytes to a monolayer of TNF-stimulated (2 ng/ml, 16 h) ECs upon stable expression of MEK5D. *F*, quantitative leukocyte adhesion assays show decreased adhesion of fluorescently labeled human THP-1 monocytes to TNF-stimulated ECs expressing MEK5D and reversion by retroviral co-expression of Erk5 shRNA. Adhesion was quantified by measuring fluorescence of total lysates at an appropriate wavelength. Data represent average-fold fluorescence values related to unstimulated pBP/pRS vector co-infected cells (arbitrarily set to 1) and are derived from three independent experiments. *ns*, not significant.

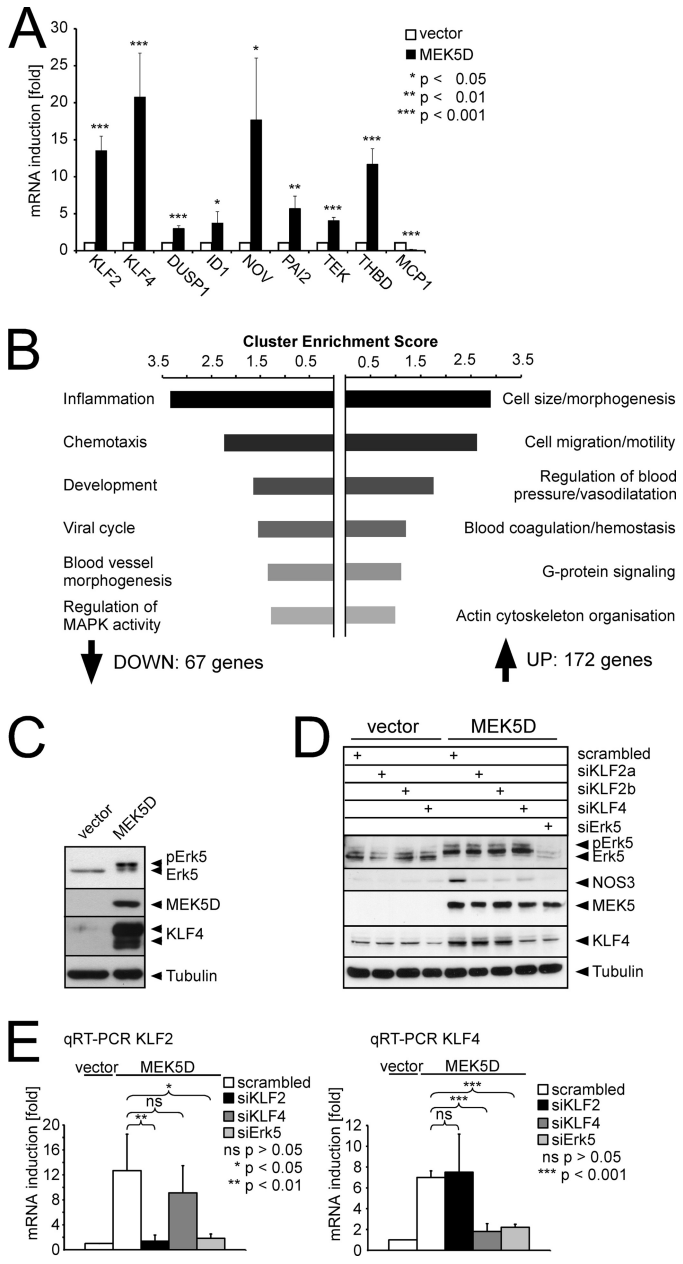

FIGURE 2. **Endothelial targets of active Erk5.** *A* and *B*, HUVECs were infected with MEK5D or control vector, and RNA was isolated 40 h post-infection. *A*, qRT-PCRs validating MEK5D-dependent expression of nine selected Erk5 targets from the microarray analysis. Relative expression of the indicated genes was normalized to glyceraldehyde-3-phosphate dehydrogenase expression and subsequently related to empty vector-infected cells (arbitrarily set to 1) to calculate -fold mRNA induction. Data show the means from three independent experiments ± S.D. *B*, bioinformatic functional annotation cluster analysis of the MEK5D-microarray data using DAVID is shown. The given enrichment score ranks the indicated functional clusters according to statistical overrepresentation of its included GO groups in relation to the totally represented genes on the chip. Only functional annotation clusters containing at least one GO group with statistically significant *p* value (<0.05) are shown. *C–E*, HUVEC were infected with empty vector or MEK5D and either lysed 96 h after infection for Western blots for verification of KLF4 protein induction (*C*) or transfected with the indicated siRNAs before infection and processed for Western blot against the indicated proteins (*D*) or for qRT-PCR analysis of KLF2 mRNA (*E*, *left*) or KLF4 mRNA expression (*E*, *right*) 40 h after infection, respectively. *ns*, not significant.

both KLF2 siRNA and KLF4 siRNA in ECs suggested that both factors mediate gene expression downstream of Erk5. To explore the relative contribution of KLF2 to gene expression downstream of Erk5, we determined the total percentage of reported KLF2 targets among the up-regulated or repressed MEK5D targets. Additionally, we analyzed its percentile distribution for the individual MEK5D-regulated functional clusters separately. For this, we compared our data set to a published microarray of direct KLF2 targets in ECs (12). We found a high representation of known KLF2 targets across the MEK5D-regulated genes (supplemental Table S2), which correlated with a high ratio of reported KLF2 targets in several of our identified functional clusters (Fig. 3*A*). However, in some clusters, in particular in the groups "Regulation of blood pressure/vasodilatation" and "Blood coagulation/hemostasis," established KLF2 targets were underrepresented with respect to the total percentages of KLF2 targets among all up- or down-regulated transcripts by MEK5D. This suggested a regulation by KLF2-independent factors. To evaluate if KLF4 could be involved, we selected several genes from different functional clusters and monitored their expression upon forced KLF4 expression. The target genes were chosen (*a*) on the basis of assignment to the specific functional annotation clusters identified by DAVID analysis (supplemental Table S1), (*b*) for exerting an established function in angiogenesis, migration, inflammation, coagulation, apoptosis or vasodilatation, or (*c*) for putative co-regulation or a likely independence of KLF2 according to published data.

Similar to MEK5D, KLF4 expression induced the expression of the vasodilatory, fibrolytic, and anti-thrombotic genes ADRB2, PLAT, and THBD. Likewise, expression levels of DUSP1, a p38-specific MAPK phosphatase recently reported to dampen endothelial inflammation via p38 inhibition (29), and the two angiogenesis/migration-related genes SEMA3F and TEK/TIE2 were up-regulated by both MEK5D and KLF4 (Fig. 3*B*). Western blots verified that both MEK5D and KLF4 further induced protein expression of ADAMTS1, PAI2/SerpinB2, NOS3, and NOV/CCN3, which are all known for their tissue-protective and -remodeling properties (Fig. 3*C*) (30–33).

Next, we tested the dependence of MEK5D-induced expression of 10 of those targets on KLF4. Therefore, MEK5D-expressing ECs were transfected with siRNA against KLF4. Depletion of KLF4 significantly reduced MEK5D-induced expression of ADAMTS1, ADRB2, NOS3, and PAI2. In contrast, only statistically insignificant mRNA reductions were observed for DUSP1, SEMA3F, and KLF2, and no expression changes were observed for the previously reported KLF2 targets PLAT, TEK, and THBD (12, 14), suggesting that MEK5D-induced regulation of those genes may depend on KLF2 (Fig. 3*D*). To evaluate this, we employed siRNA against KLF2. With the exception of TEK and SEMA3F, all those non-significantly siKLF4-regulated MEK5D targets were significantly reduced by KLF2 depletion (Fig. 3*D*). Overall, these data indicate that KLF2 and KLF4 can principally co-regulate several of their targets but obviously still exhibit certain target specificity due to individual differences in their affinities for jointly regulated promoters.

Effects of KLF4 on Inflammation, Survival, Migration, and Angiogenesis—To evaluate a potential involvement of KLF4 in downstream responses to Erk5 activation, we analyzed the functional consequences of KLF4 and MEK5D expression side by side. We first concentrated on the anti-inflammatory effect

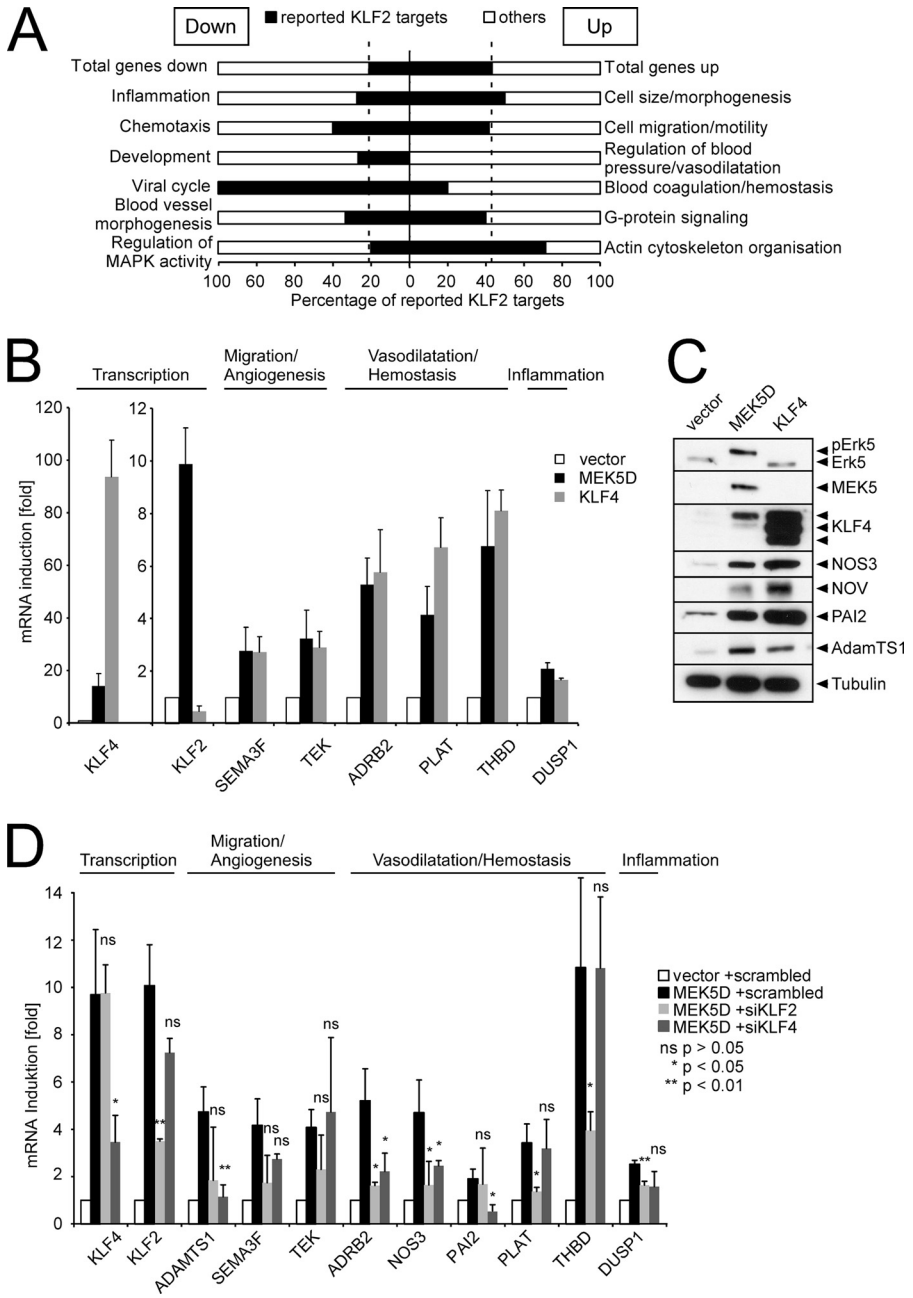

FIGURE 3. **KLF4 regulates gene expression downstream of Erk5.** *A*, a representation is shown depicting the percentage of reported KLF2 target genes among the MEK5D-regulated functional annotation clusters as identified by comparison of our data set of MEK5D-regulated genes to microarray data of published endothelial KLF2 targets (12). The *bars* indicate the percentages of reported KLF2 targets (*black*) or putatively KLF2-independent genes (*other*, *non-filled*) calculated for all up- and down-regulated genes (*top*) or for the individual MEK5D-regulated functional clusters, respectively. The total percentages of reported KLF2 targets for the overall 172 up-regulated/induced genes and 67 repressed transcripts identified by our MEK5D microarray is indicated by *dashed lines* for comparison. *B–D*, HUVECs were retrovirally infected as indicated and processed differently for the individual experiments. *B*, RNA samples were taken 40 h post-infection and subjected to qRT-PCR for quantification of -fold mRNA expression of the indicated genes related to control vector-infected cells. Data display average values from three experiments ±S.D. *C*, cells were treated overnight with 2 μM monensin to prevent release of extracellular proteins (*e.g.* ADAMTS1, PAI2, and NOV), lysed 40 h after infection, and analyzed by Western blot using specific antisera against the identified MEK5D target proteins. Tubulin served as loading control. *D*, HUVECs were transfected with siRNA against KLF2, KLF4, or scrambled siRNA 4 h before infection with empty vector or MEK5D. Expression of the indicated genes was monitored 40 h post-infection by qRT-PCR as described in *B*. Additionally, in *B* and *D* a functional classification of the genes based on published evidence or assignment to specific functional annotation clusters identified by the DAVID algorithm is indicated. *ns*, not significant.

of MEK5D as KLF4 has previously been shown to inhibit pro-inflammatory gene expression in ECs (27). In this report KLF4 overexpression resulted in decreased TNF-mediated leukocyte adhesion associated with reduced expression of the cell adhesion molecule VCAM1. Thus, we first confirmed the anti-adhesive effect of KLF4 in quantitative adhesion assays and by measurement of TNF-induced VCAM1 induction by flow cytometry. Similar to Erk5 (compare Fig. 1*F*), KLF4 expression repressed TNF-induced leukocyte adhesion (supplemental Fig. S1*A*), and both MEK5D and KLF4 expression strongly inhibited TNF-induced VCAM1 expression at the protein and mRNA levels (supplemental Fig. S1*B* and Fig. 4*A*).

Expression of pro-inflammatory genes such as VCAM1 is strictly dependent on activation of the pro-inflammatory IKK2/NFκB cascade in ECs (23). NFκB activation commonly is triggered by IKK2-mediated degradation of IκB, an inhibitory protein that in the absence of IKK2 activity prevents NFκB activation by sequestering it in the cytoplasm. Alternatively, NFκB activity can directly be modulated at the level of transactivation, *e.g.* by altering acetylation of nuclear NFκB (34), which is required for optimal transcription of various TNF-induced target genes including VCAM1 in ECs (35). To discriminate between both possibilities, we first evaluated whether IκB degradation was altered upon expression of MEK5D or KLF4. Fig. 4*B* illustrates that degradation of the NFκB-inhibitory protein IκB was unchanged by expression of active MEK5 or KLF4 compared with vector-infected cells, suggesting that cytoplasmic steps of NFκB activation such as IKK2 activation were not impaired. However, in luciferase assays using a 6× κB-driven luciferase reporter gene, a ~50% decrease of TNF-induced NFκB activity was observed (Fig. 4*C*). Thus, inhibition of NFκB-dependent gene expression appears to occur at the level of transactivation. In agreement, expression of MEK5D or KLF4 compromised TNF-induced protein induction of other established NFκB-dependent target genes such as MCP1 or interleukin-8 (Fig. 4*D*).

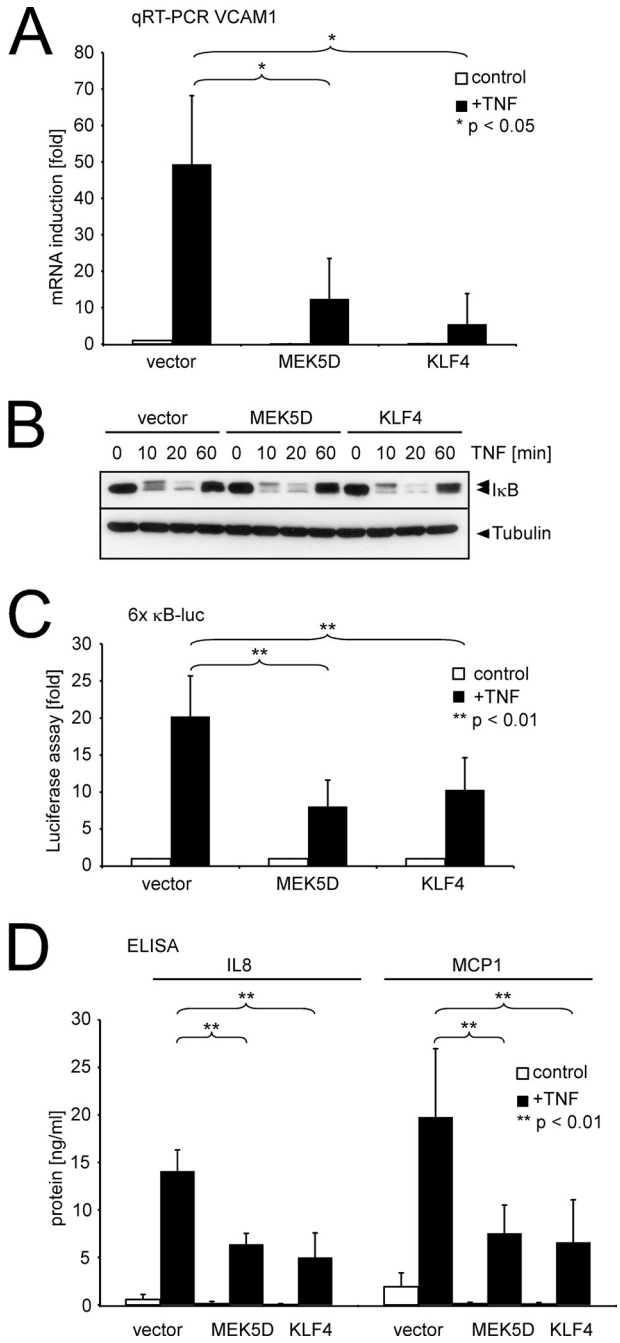

FIGURE 4. **Expression of KLF4 and MEK5D suppresses TNF-induced inflammatory responses by inhibiting NFκB-dependent gene expression at the level of transactivation.** HUVECs were retrovirally infected with empty vector, MEK5D, or KLF4, puromycin-selected, and reseeded for the respective experiments. *A*, qRT-PCR data for VCAM1, demonstrating statistically significant reduction of TNF-induced VCAM1 mRNA upon expression of KLF4 or MEK5D are shown. *B*, expression of KLF4 and MEK5D does not alter the kinetics of TNF-induced IκBα degradation. Cells were stimulated with TNF for the indicated time points, and total lysates were examined for IκBα protein degradation by Western blot. *C*, expression of KLF4 or MEK5D inhibits activity of a NFκB-dependent luciferase reporter. The differently infected HUVECs were co-transfected with a NFκB-responsive 6× κB-firefly luciferase and a renilla-luciferase reporter, and luciferase activities were measured 16 h after stimulation with medium or TNF in a luminometer. The data represent -fold ratios of firefly/renilla activities ± S.D. related to unstimulated empty vector-infected cells, which were arbitrarily set to 1. *D*, enzyme-linked immunosorbent assays (*ELISA*) show decreased protein levels of the NFκB-dependent proinflammatory cytokines interleukin-8 (*IL8*) and MCP1 in the culture supernatants of TNF-stimulated HUVEC stably expressing KLF4 or MEK5D, respectively. Data in *A*, *C*, and *D* are derived from 3–5 independent experiments and show average values ±S.D.

We next compared the anti-apoptotic properties of MEK5D and its signal transducer KLF4. Interestingly, expression of KLF4 similarly reduced both basal apoptosis as well as apoptosis induction triggered by growth factor deprivation. This was evident by a comparable repression of basal as well as deprivation-induced cleavage of the executioner caspase-3 in Western blots and an equally effective reduction of subdiploidy of KLF4-infected cells in parallel DNA profiling experiments (Fig. 5, *A* and *B*). Similar to stable MEK5D introduction, KLF4 expression also strongly inhibited basal as well as VEGF-induced sprouting in three-dimensional spheroid assays (Fig. 5*C*) and negatively affected the migratory potential of ECs in separate migration arrays (Fig. 5*D*). Overall, these data confirm that KLF4 expression can recapitulate several protective effects of active Erk5.

Protective Drugs of the Statin Family Induce Activation of the MEK5/Erk5/KLF4 Cascade—Given that constitutive Erk5 activation results in a protective gene expression pattern, we evaluated the possibility that vasoprotective drugs might mediate their responses via Erk5. Among the drugs used for treatment of various vascular diseases, 3-hydroxy-3-methylglutaryl-coenzyme A reductase inhibitors of the statin group have attained great attention due to their vasodilatory, immunosuppressive, anti-thrombotic, and cholesterol-decreasing capabilities (36). We, thus, tested whether treatment of ECs with statins might activate Erk5. Indeed, Western blots revealed that treatment with three different statins potently induced Erk5 phosphorylation (Fig. 6*A*). Remarkably, statin treatment also increased protein expression of KLF4 and its confirmed targets ADAMTS1 and NOS3 in ECs (Fig. 6*A*), suggesting that statins may mediate at least some of their protective effects via the Erk5/KLF4 axis. Titration experiments revealed that simvastatin could consistently increase KLF4 mRNA expression and NOS3 protein production at concentrations as little as ~1 μM (Fig. 6*B*), a concentration previously shown to inhibit proinflammatory gene expression in ECs (37). Of note, these effects strictly correlated with Erk5 phosphorylation, which first became apparent at around 0.5–1 μM and reached its maximum at 5–10 μM (Fig. 6*B*). To confirm the dependence of statin-induced KLF4 induction on the MEK5/Erk5 module, we knocked down both mRNAs employing RNAi. Indeed, siRNA against MEK5 strongly decreased simvastatin-induced KLF4 mRNA expression (Fig. 6*C*). Consistently, shRNA-induced depletion of Erk5 blunted the effect of simvastatin to induce KLF4 mRNA and protein expression, demonstrating that Erk5 activation is indispensable for statin-induced KLF4 induction (Fig. 6, *D* and *E*). In agreement, shRNA against Erk5 inhibited simvastatin-induced expression of the KLF4 targets ADAMTS1 and NOS3 at the mRNA and protein level (Fig. 6, *D* and *E*). The latter was also observed by KLF4 siRNA, confirming that simvastatin-dependent gene expression is at least partially mediated via Erk5 and KLF4 (Fig. 6*F*).

DISCUSSION

A variety of stimuli have been reported to activate Erk5 in different cells. Here we provide evidence that constitutive activation of Erk5 in ECs results in an overall protective phenotype characterized by increased apoptosis resistance and a decreased angiogenic, migratory, and pro-inflammatory poten-

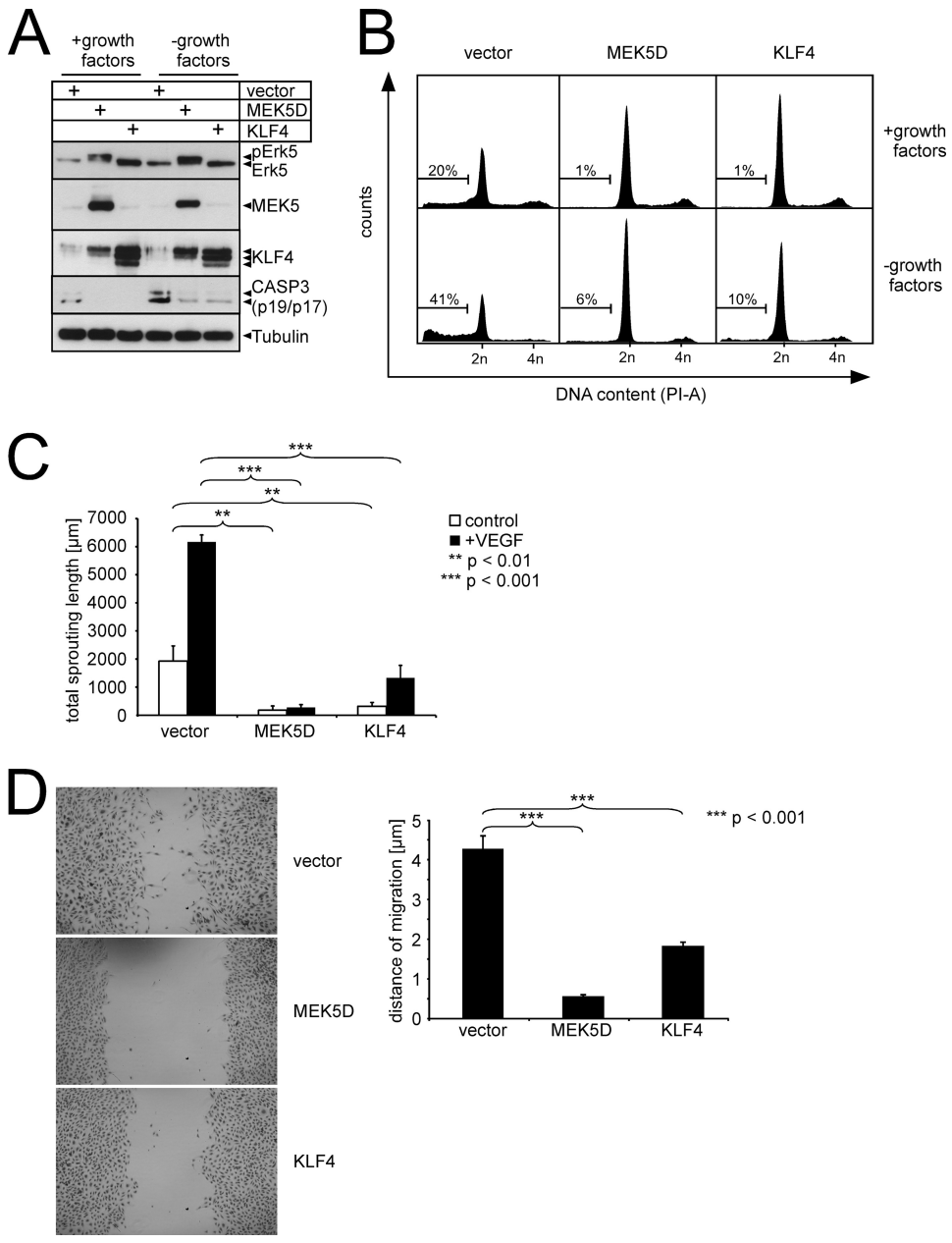

FIGURE 5. **KLF4 overexpression mimics the anti-apoptotic and anti-angiogenic effects of active Erk5.** HUVECs were retrovirally infected with MEK5D, KLF4, or control vector. Except for *C*, cells were puromycin-selected 72 h post-infection and reseeded for the individual experiments. *A* and *B*, cells were deprived of growth factors and fetal bovine serum for 48 h or incubated in normal growth medium for 48 h. Apoptosis induction was monitored by detection of cleaved caspase-3 (*Casp3*) using a cleavage-specific antiserum (*A*) or analyzed by measuring subdiploid DNA content of PI-stained cells by flow cytometry (*B*). Western blots for MEK5, KLF4, and tubulin in *A* served as expression or loading controls, respectively. Additionally, an immunoblot for Erk5 is shown to confirm activity of the expressed MEK5D construct. *C*, shown is decreased basal and VEGF-induced angiogenic sprouting of MEK5D- or KLF4-infected HUVECs as determined in three-dimensional-sprouting assays. Data represent quantifications of the average total sprouting length of each 10 spheroids from three independent experiments ±S.D. The spheroids were seeded into collagen and stimulated with 10 ng/ml VEGF or medium alone for 24 h. *D*, *left*, microscopic images show decreased migration capacity of the KLF4- and MEK5D-expressing cells as determined by wounding assay. Images are taken 16 h after infliction of the damage. *Right*, measurement of the averaged distances of migration ± S.D. obtained for the differently infected cells is shown. Data are averaged from five experiments.

tial. All these effects have also been ascribed to laminar flow, which can activate the MEK5/Erk5 pathway in ECs (3), suggesting that fluid shear stress acts as the major physiological stimulus of the MEK5/Erk5 pathway in ECs. In favor of this hypothesis, bioinformatic analysis of our microarray data reflected the protective effects of Erk5 observed *in vitro* and additionally revealed an immunosuppressive, anti-thrombotic, and vasodilatory function of the MEK5/Erk5 pathway. Of note, we did not observe an overrepresentation of general stress-response genes and immediate early genes, which usually indicate general growth factor-induced or stress-induced responses, excluding a high degree of unspecific gene expression induced by constitutive Erk5 activation.

In agreement with a current report, which revealed KLF4 regulation by MEK5D in qRT-PCR experiments (38), we identified KLF4 as target gene of MEK5D. Surprisingly, however, this group failed to detect KLF4 regulation in transcription profiling analysis of MEK5D targets and claimed Erk5-independent regulation of KLF4 by MEK5 as Erk5 siRNA did not affect its induction in their experiments. In contrast to these partially inconsistent data, our microarray revealed KLF4 as the topmost-regulated gene by MEK5D, and our Erk5 shRNA experiments clearly confirmed its regulation via Erk5. Unlike the study by Villarreal *et al.* (38), who did not provide functional assays confirming a role of KLF4 downstream of the MEK5/Erk5 pathway, our data demonstrate that forced KLF4 expression can recapitulate virtually all observed vasoprotective responses downstream of Erk5. Notably, our data also revealed a suppressive effect of KLF4 on endothelial migration and angiogenesis, which has not been described before. Moreover, our KLF4 siRNA experiments clearly show a contribution of KLF4 to Erk5-dependent expression of a variety of functional relevant genes. Thus, our data not only prove that KLF4 is located downstream of Erk5 but also demonstrate that it indeed represents a functionally relevant mediator of Erk5-dependent gene expression in ECs. In agreement with that, KLF4 has previously been identified in a microarray study for flow-activated genes (28) and is known to suppress proinflammatory gene expression in ECs (27). It should be noted, however, that consistent with a study in Erk5-deficient mouse embryonic fibroblasts (26), we additionally identified KLF2 as major factor induced

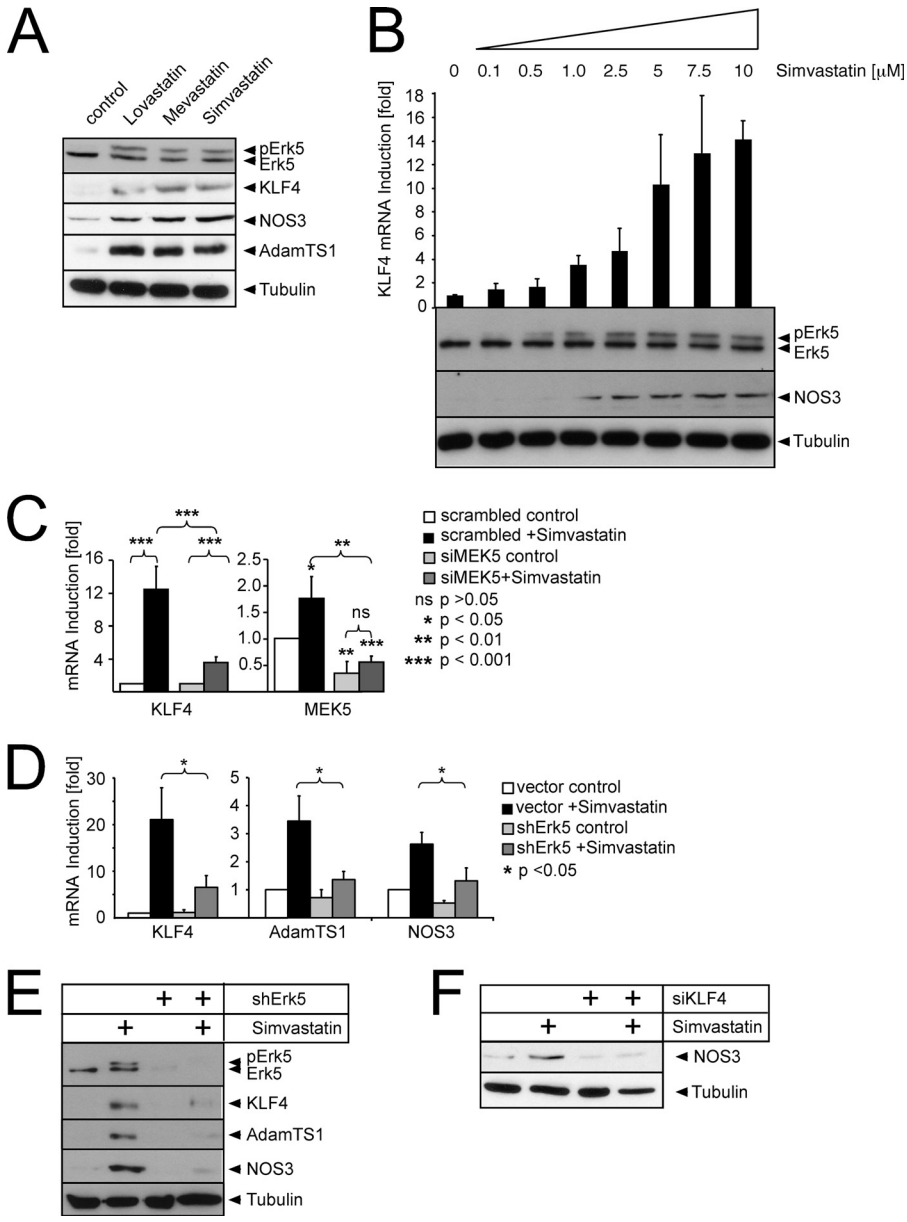

FIGURE 6. **Statins induce KLF4 and KLF4-dependent gene expression via activation of Erk5.** HUVECs were treated with each 10 μM concentrations of the indicated statins for 24 h unless indicated otherwise. *A*, Erk5 phosphorylation and expression of KLF4 and its targets NOS3 and ADAMTS1 were determined by Western blot. Tubulin served as the loading control. *B*, simvastatin triggers Erk5 phosphorylation and induction of KLF4 mRNA and NOS3 protein in a concentration-dependent manner. *Bars* show qRT-PCR experiments for KLF4 averaged from three experiments ±S.D. An immunoblot for tubulin is shown to indicate equal loading of the lanes for Erk5 and NOS3, respectively. *C*, *left panel*, suppression of simvastatin-induced KLF4 mRNA production upon transfection with siRNA against MEK5 is shown. Data represent the averages of three independent qRT-PCR experiments ±S.D. For control of knockdown levels, the respective qRT-PCRs for MEK5 are shown (*right panel*). *D*, qRT-PCR data for KLF4, ADAMTS1, and NOS3 reveal mRNA induction by simvastatin and reversion by expression of shRNA against Erk5. *E*, depletion of Erk5 prevents simvastatin-induced protein expression of NOS3 and ADAMTS1. *F*, transfection of siRNA against KLF4 reduces simvastatin-induced NOS3 protein production.

by active MEK5D. KLF2 is known to control flow-dependent gene expression (12, 13), and its overexpression has likewise been shown to elicit various vasoprotective responses in ECs (14, 15, 39), leading to the conclusion that KLF2 mediates a significant portion of the gene expression downstream of Erk5. In fact, comparison of our data set to that of Parmar *et al.* (12), who published a transcriptional profiling study of KLF2 targets in HUVEC, revealed a high representation of reported KLF2 targets among the MEK5D-induced genes (supplemental Table S2 and Fig. 3*A*). However, KLF4 expression could regulate a wide variety of MEK5D targets in our qRT-PCR experiments, including previously reported KLF2 targets such as NOS3 and THBD. This suggests that KLF2 and KLF4 act partially redundant in ECs. This is also supported by a recent study that previously reported induction of established KLF2 targets by KLF4 in ECs (27). Moreover, another study showed a compensatory upregulation of KLF4 upon deletion of one KLF2 allele, which has been suggested to account for the absent endothelial phenotype upon partial KLF2 loss (39). These data predict that at least some of the reported KLF2 targets can be co-regulated by KLF4 or may even be preferentially controlled by KLF4 under physiological conditions. Our siRNA data underscore this assumption; we demonstrate that maximal induction of NOS3 by MEK5D requires both KLF2 and KLF4. This was evident by a statistically significant reduction of MEK5D-induced NOS3 expression by both KLF2 siRNA and KLF4 siRNA. Furthermore, MEK5D-dependent induction of other genes, such as the established KLF2 target THBD, was significantly affected by KLF2 siRNA but not KLF4 siRNA, albeit THBD was robustly induced by KLF4 overexpression. Conversely, expression of ADAMTS1 and PAI2, which exert anti-angiogenic (33) and anti-apoptotic functions (40), is not significantly affected by KLF2 siRNA but strongly reduced by KLF4 siRNA. Thus, in addition to a partial redundancy, each KLF appears to have its preferential targets.

In direct comparison, MEK5D and KLF4 similarly suppressed TNF-induced activation of a 6× NFκB-luc promoter without affecting IκB degradation. This indicates that MEK5D and KLF4 do not mediate their anti-inflammatory effects by interfering with receptor activation or modulation of IKK2 activity. Rather, they inhibit NFκB activation at the level of transactivation, which is strongly dependent on co-stimulatory signals such as p38 activation, which affects acetylation of NFκB (34) and, importantly, amplifies NFκB-induced proinflammatory gene expression in ECs (35). For KLF4, similar conclusions were drawn by Hamik *et al.* (27), who observed that

KLF4 expression did not affect NFκB binding in band-shift assays in ECs but reduced NFκB activity by about 50% in luciferase assays in COS cells. Although the authors did not provide a mechanism, KLF4 has been reported to bind the transcriptional co-activator p300/CBP (41, 42), and p300/CBP-mediated acetylation of NFκB is required for optimal transactivation of NFκB-dependent target genes (43). Thus, in analogy to its reported inhibitory effect on TGF-β-induced gene expression in colon epithelial cells in which KLF4 blocks β-catenin acetylation by CBP/p300 (44), KLF4 might mediate its effects on NFκB activity by modulating acetylation.

Consistent with the overall protective gene response, we show that statins can potently activate Erk5 and induce KLF4 and KLF4-dependent gene expression. Although these vasoprotective drugs have initially been identified as 3-hydroxy-3-methylglutaryl-coenzyme A reductase inhibitors (45), statins also exert other beneficial effects beyond their lipid-lowering capacity (36, 46, 47). Mechanistically, they prevent isoprenylation and membrane localization of small-G proteins such as RhoA, thereby inhibiting their activation. Intriguingly, RhoA activation is a major mechanism to limit NOS3 production and accordingly NO levels in cells, which is antagonized by statins (36, 46). Although others have previously shown a role for KLF2 in this process (48, 49), a recent report has also implicated a potential function of KLF4, as it is likewise induced by statins (38). Consistently, our RNAi experiments demonstrate a central role of Erk5 and KLF4 in statin-induced NOS3 production and other transcriptional responses to statins. Although it is currently unclear how exactly Erk5 is activated by statins, we speculate that inhibition of small GTPases is responsible for that. This hypothesis is corroborated by the overrepresentation of the functional cluster *G-Protein signaling* (see Fig. 2*B*) among the MEK5D-induced genes. Experiments are currently under way to further elucidate the mechanism of statin-induced Erk5 activation.

In summary, our data provide evidence that the MEK5/Erk5 pathway plays critical roles in vasoprotection and present KLF4 as key mediator in this process. Considering the potent inhibitory effects of MEK5D and KLF4 on angiogenic, inflammatory, and thrombotic gene expression, our data further suggest agonists of the MEK5/Erk5/KLF4 module of potential therapeutic value for treatment of vascular diseases and as regiment against tumor angiogenesis. Future studies, including *in vivo* models, are mandatory to explore such approaches.

Acknowledgments—We thank Annika Huss and Silke Garkisch for excellent technical assistance.

REFERENCES

1. Traub, O., and Berk, B. C. (1998) *Arterioscler. Thromb. Vasc. Biol.* **18,** 677–685
2. Hayashi, M., and Lee, J. D. (2004) *J. Mol. Med.* **82,** 800–808
3. Yan, C., Takahashi, M., Okuda, M., Lee, J. D., and Berk, B. C. (1999) *J. Biol. Chem.* **274,** 143–150
4. Nishimoto, S., and Nishida, E. (2006) *EMBO Rep.* **7,** 782–786
5. Nakamura, K., Uhlik, M. T., Johnson, N. L., Hahn, K. M., and Johnson, G. L. (2006) *Mol. Cell. Biol.* **26,** 2065–2079
6. Kato, Y., Kravchenko, V. V., Tapping, R. I., Han, J., Ulevitch, R. J., and Lee, J. D. (1997) *EMBO J.* **16,** 7054–7066
7. Kasler, H. G., Victoria, J., Duramad, O., and Winoto, A. (2000) *Mol. Cell. Biol.* **20,** 8382–8389
8. Regan, C. P., Li, W., Boucher, D. M., Spatz, S., Su, M. S., and Kuida, K. (2002) *Proc. Natl. Acad. Sci. U.S.A.* **99,** 9248–9253
9. Sohn, S. J., Sarvis, B. K., Cado, D., and Winoto, A. (2002) *J. Biol. Chem.* **277,** 43344–43351
10. Yan, L., Carr, J., Ashby, P. R., Murry-Tait, V., Thompson, C., and Arthur, J. S. (2003) *BMC Dev. Biol.* **3,** 11
11. Akaike, M., Che, W., Marmarosh, N. L., Ohta, S., Osawa, M., Ding, B., Berk, B. C., Yan, C., and Abe, J. (2004) *Mol. Cell. Biol.* **24,** 8691–8704
12. Parmar, K. M., Larman, H. B., Dai, G., Zhang, Y., Wang, E. T., Moorthy, S. N., Kratz, J. R., Lin, Z., Jain, M. K., Gimbrone, M. A., Jr., and García-Cardeña, G. (2006) *J. Clin. Invest.* **116,** 49–58
13. Dekker, R. J., Boon, R. A., Rondaij, M. G., Kragt, A., Volger, O. L., Elderkamp, Y. W., Meijers, J. C., Voorberg, J., Pannekoek, H., and Horrevoets, A. J. (2006) *Blood* **107,** 4354–4363
14. Lin, Z., Kumar, A., SenBanerjee, S., Staniszewski, K., Parmar, K., Vaughan, D. E., Gimbrone, M. A., Jr., Balasubramanian, V., García-Cardeña, G., and Jain, M. K. (2005) *Circ. Res.* **96,** e48–57
15. SenBanerjee, S., Lin, Z., Atkins, G. B., Greif, D. M., Rao, R. M., Kumar, A., Feinberg, M. W., Chen, Z., Simon, D. I., Luscinskas, F. W., Michel, T. M., Gimbrone, M. A., Jr., García-Cardeña, G., and Jain, M. K. (2004) *J. Exp. Med.* **199,** 1305–1315
16. Abe, J., Kusuhara, M., Ulevitch, R. J., Berk, B. C., and Lee, J. D. (1996) *J. Biol. Chem.* **271,** 16586–16590
17. Dinev, D., Jordan, B. W., Neufeld, B., Lee, J. D., Lindemann, D., Rapp, U. R., and Ludwig, S. (2001) *EMBO Rep.* **2,** 829–834
18. Brummelkamp, T. R., Bernards, R., and Agami, R. (2002) *Cancer Cell* **2,** 243–247
19. Müller, V., Viemann, D., Schmidt, M., Endres, N., Ludwig, S., Leverkus, M., Roth, J., and Goebeler, M. (2007) *J. Immunol.* **179,** 8435–8445
20. Viemann, D., Schmidt, M., Tenbrock, K., Schmid, S., Müller, V., Klimmek, K., Ludwig, S., Roth, J., and Goebeler, M. (2007) *J. Immunol.* **178,** 3198–3207
21. Huang da, W., Sherman, B. T., and Lempicki, R. A. (2009) *Nat. Protoc.* **4,** 44–57
22. Spiering, D., Schmolke, M., Ohnesorge, N., Schmidt, M., Goebeler, M., Wegener, J., Wixler, V., and Ludwig, S. (2009) *J. Biol. Chem.* **284,** 24972–24980
23. Denk, A., Goebeler, M., Schmid, S., Berberich, I., Ritz, O., Lindemann, D., Ludwig, S., and Wirth, T. (2001) *J. Biol. Chem.* **276,** 28451–28458
24. Bielenberg, D. R., Hida, Y., Shimizu, A., Kaipainen, A., Kreuter, M., Kim, C. C., and Klagsbrun, M. (2004) *J. Clin. Invest.* **114,** 1260–1271
25. Guttmann-Raviv, N., Shraga-Heled, N., Varshavsky, A., Guimaraes-Sternberg, C., Kessler, O., and Neufeld, G. (2007) *J. Biol. Chem.* **282,** 26294–26305
26. Sohn, S. J., Li, D., Lee, L. K., and Winoto, A. (2005) *Mol. Cell. Biol.* **25,** 8553–8566
27. Hamik, A., Lin, Z., Kumar, A., Balcells, M., Sinha, S., Katz, J., Feinberg, M. W., Gerzsten, R. E., Edelman, E. R., and Jain, M. K. (2007) *J. Biol. Chem.* **282,** 13769–13779
28. McCormick, S. M., Eskin, S. G., McIntire, L. V., Teng, C. L., Lu, C. M., Russell, C. G., and Chittur, K. K. (2001) *Proc. Natl. Acad. Sci. U.S.A.* **98,** 8955–8960
29. Zakkar, M., Chaudhury, H., Sandvik, G., Enesa, K., Luong le, A., Cuhlmann, S., Mason, J. C., Krams, R., Clark, A. R., Haskard, D. O., and Evans, P. C. (2008) *Circ. Res.* **103,** 726–732
30. Croucher, D. R., Saunders, D. N., Lobov, S., and Ranson, M. (2008) *Nat. Rev. Cancer* **8,** 535–545
31. Katsube, K., Sakamoto, K., Tamamura, Y., and Yamaguchi, A. (2009) *Dev. Growth Differ.* **51,** 55–67
32. Kawashima, S., and Yokoyama, M. (2004) *Arterioscler. Thromb. Vasc. Biol.* **24,** 998–1005
33. Vázquez, F., Hastings, G., Ortega, M. A., Lane, T. F., Oikemus, S., Lombardo, M., and Iruela-Arispe, M. L. (1999) *J. Biol. Chem.* **274,** 23349–23357
34. Perkins, N. D. (2007) *Nat. Rev. Mol. Cell Biol.* **8,** 49–62
35. Viemann, D., Goebeler, M., Schmid, S., Klimmek, K., Sorg, C., Ludwig, S.,

and Roth, J. (2004) *Blood* **103,** 3365–3373
36. Schönbeck, U., and Libby, P. (2004) *Circulation* **109,** II18–26
37. Eccles, K. A., Sowden, H., Porter, K. E., Parkin, S. M., Homer-Vanniasinkam, S., and Graham, A. M. (2008) *Atherosclerosis* **200,** 69–79
38. Villarreal, G., Jr., Zhang, Y., Larman, H. B., Gracia-Sancho, J., Koo, A., and García-Cardeña, G. (2010) *Biochem. Biophys. Res. Commun.* **391,** 984–989
39. Atkins, G. B., Wang, Y., Mahabeleshwar, G. H., Shi, H., Gao, H., Kawanami, D., Natesan, V., Lin, Z., Simon, D. I., and Jain, M. K. (2008) *Circ. Res.* **103,** 690–693
40. Tonnetti, L., Netzel-Arnett, S., Darnell, G. A., Hayes, T., Buzza, M. S., Anglin, I. E., Suhrbier, A., and Antalis, T. M. (2008) *Cancer Res.* **68,** 5648–5657
41. Evans, P. M., Zhang, W., Chen, X., Yang, J., Bhakat, K. K., and Liu, C. (2007) *J. Biol. Chem.* **282,** 33994–34002
42. Geiman, D. E., Ton-That, H., Johnson, J. M., and Yang, V. W. (2000) *Nucleic Acids Res.* **28,** 1106–1113
43. Chen, L. F., Mu, Y., and Greene, W. C. (2002) *EMBO J.* **21,** 6539–6548
44. Evans, P. M., Chen, X., Zhang, W., and Liu, C. (2009) *Mol. Cell. Biol.* **30,** 372–381
45. Libby, P. (2002) *Nature* **420,** 868–874
46. Ludman, A., Venugopal, V., Yellon, D. M., and Hausenloy, D. J. (2009) *Pharmacol. Ther.* **122,** 30–43
47. Greenwood, J., and Mason, J. C. (2007) *Trends Immunol.* **28,** 88–98
48. Parmar, K. M., Nambudiri, V., Dai, G., Larman, H. B., Gimbrone, M. A., Jr., and García-Cardeña, G. (2005) *J. Biol. Chem.* **280,** 26714–26719
49. Sen-Banerjee, S., Mir, S., Lin, Z., Hamik, A., Atkins, G. B., Das, H., Banerjee, P., Kumar, A., and Jain, M. K. (2005) *Circulation* **112,** 720–726